Article

Investigation of the Effects of Infrared and Hot Air Oven Drying Methods on Drying Behaviour and Colour Parameters of Red Delicious Apple Slices

Oldřich Dajbych [ID], Abraham Kabutey *[ID], Čestmír Mizera and David Herák [ID]

Department of Mechanical Engineering, Faculty of Engineering, Czech University of Life Sciences Prague, 165 00 Prague, Czech Republic; dajbych@tf.czu.cz (O.D.); mizera@tf.czu.cz (Č.M.); herak@tf.czu.cz (D.H.)
* Correspondence: kabutey@tf.czu.cz; Tel.: +420-22438-3180

Abstract: This present study investigated thin-layer drying characteristics of dried apple slices for a range of temperatures from 40 °C to 80 °C at a constant drying time of 10 h under infrared (IR) and hot air oven (OV) drying methods. The fresh apples were cut into a cylindrical size of thickness of 8.07 ± 0.05 mm and a diameter of 66.27 ± 3.13 mm. Fourteen thin-layer mathematical models available in the literature were used to predict the drying process. The goodness of fit of the drying models was assessed by the root mean square error (RMSE), chi-square (χ^2), coefficient of determination (R^2) and modelling efficiency (EF). The results showed that the lightness and greenness/redness of the dried sample, total colour change, chroma change, colour index, whiteness index, bulk density, final surface area and final volume significantly (p-value < 0.05) correlated with the drying temperature under IR. Under OV, however, only the final surface area and bulk density of the dried samples showed significant (p-value < 0.05) with the drying temperature. Shrinkage values for OV and IR methods showed both increasing and decreasing trends along with the drying temperatures. The Weibull distribution model proved most suitable for describing the drying processes based on the statistical validation metrics of the goodness of fit. In future studies, the combined effect of the above-mentioned drying methods and other drying techniques on apple slices among other agricultural products should be examined to obtain a better insight into the drying operations and quality improvement of the final product for preservation and consumer acceptability.

Keywords: agricultural product; drying behaviour; shrinkage; rehydration capacity; empirical models

1. Introduction

Apple (*Malus domestica* Borkh) belongs to the Rosaceae family which is the fourth most consumed fresh fruit worldwide due to its flavor and high nutritional value [1–4]. It can be eaten in various forms such as dried, juice, jam or marmalade [5,6]. The regular consumption of apples prevents neurodegenerative diseases and reduces the risk of asthma [4,7–9].

The high moisture content of stored foods such as apples is the primary cause of storage mould growth [10]. Drying of agricultural products is done to reduce the moisture content through evaporating and sublimation processes, including heat and mass transfer mechanisms [10–15]. It inhibits microbial, enzymatic and quality decay [13,15,16]. It can also impact the quality, texture and nutritional value of the final product and increase the shelf life [6,13,15]. Consumers' preference for dried products is based on their physical qualities such as colour, shape, aroma and appearance [15,17].

In the literature, several studies have been conducted on the thin-layer drying characteristics of fruits and vegetables using different drying methods [4,10,11,13,18–29]. Thin-layer drying is the procedure of drying one single layer of particles or slices of a product [30]. For instance, Aral and Bese [16] studied the thin-layer drying characteristics of hawthorn fruit using a convective dryer at different air temperatures between 50 °C and 70 °C and air

velocities between 0.5 and 1.3 m/s. The authors found that the drying time decreased with increasing air temperature and velocity. Jafari et al. [11] examined the effect of the thickness of samples, air velocity and infrared power on the drying kinetics and quality attributes of blanched eggplant slices during infrared drying. Wang et al. [18] also explored the effects of three drying methods (air impingement drying, AID; infrared-assisted hot air drying, IR-HAD; hot-air drying based on temperature and humidity control, TH-HAD) on physico-chemical properties, drying kinetics, microstructure and specific energy consumption of potato cubes. The authors indicated that TH-HAD had the shortest drying time followed by IR-HAD and AID. In addition, their results showed that the drying method significantly affected the overall quality of dried potato cubes. In addition, Li et al. [23] studied the drying rate, colour, texture, shrinkage and microstructure of *Cistanche deserticola* under hot air drying, infrared drying, freeze drying and microwave vacuum freeze drying. Their results showed that microwave freeze drying had the highest drying rate and required the shortest drying time followed by infrared drying and hot air drying.

In recent years, various drying technologies have emerged to produce dried foods. These techniques include air jet impingement combined with radio frequency and hot air drying [31]. Air jet impingement is an effective drying method in which the air impinges on the product surface at high velocity by removing thermal boundary layers of moisture and thus increases the heat transfer rate [31,32]. Radiofrequency refers to the use of electromagnetic waves of a certain frequency (3 kHz–300 MHz) to generate heat inside food materials [31,33]. Electrohydrodynamic technology is another potential method for apple drying which applies high voltage to enhance single-phase convective heat and mass transfer [34,35]. Low-frequency ultrasound, pulsed electric fields, high-pressure processing, microwaves, microwave-vacuum, ultrasound, microwave freeze drying, ultrasound-vacuum, pulsed lights, ultrasound-infrared radiation, catalytic infrared radiation and intermittent-microwave convective drying are emerging technologies or combined techniques for drying agricultural products [18,21,23,36–43].

Drying models are useful in the design, construction, process optimization and for predicting the drying behaviour under given processing conditions [15,30]. Some studies have been reported on the thin-layer drying kinetics and mathematical modeling of apple varieties such as Royal Gala, Golab, Golden, Organic, Granny Smith, Starkrimson, Florina and Golden Delicious [13,15,30,44–48]. Menges and Ertekin [44] studied the effect of drying air temperature and velocity on golden apples using a laboratory dryer. The authors applied fourteen thin-layer drying models to describe the obtained experimental drying curves. Sacilik and Elicin [13] examined the effect of drying air temperature and slice thickness on the drying characteristics and quality parameters of dried organic slices in a convective hot air dryer. The authors applied ten thin-layer drying models to the experimental drying curves. Meisami-asl et al. [45] studied thin layer drying kinetics of apple slices (Golab variety) at different temperatures, velocities and thickness using a convective dryer. The authors applied twelve different thin-layer drying models to describe the experimental drying curves. Zhu et al.'s [46] study investigated the effects of processing factors on the blanching and dehydration characteristics of apple slices exposed to simultaneous infrared dry-blanching and dehydration with intermittent heating. The authors established mathematical relationships between processing factors and product quality by using empirical modeling methods. Blanco-Cano et al. [30] described the thin-layer drying kinetics of Granny Smith apples by thermogravimetric analysis of the drying process with variable drying temperatures. The authors applied eleven different thin-layer drying equations to the experimental drying curves. Das and Akpinar [47] investigated the thermal performance of a solar air dryer with a solar tracking system of Golden Delicious cut apple slices of 14 mm thickness. The authors [47] applied nine thin-layer drying models to describe the drying curves. Aradwad et al. [15] studied the effect of drying and colour kinetics, texture, rehydration and microstructure on dried apple slices using infrared and hot air drying techniques. The authors [15] applied nine mathematical models to describe

the drying behaviour. The authors [15] further indicated that drying time, colour change and energy consumption were lower in infrared drying than in hot air drying.

In this present study, oven drying (OV) also called convective drying or hot air drying (HAD) and infrared drying (IR) are considered. OV/HAD is one of the most commonly used drying methods for agricultural products due to its many advantages, including simplicity in design, ease of operation, low operating cost and operation with a wide range of applicability [6,15,25,49–54]. However, its disadvantages are extensive, including drying time, variable temperature exposure, material hardening and significant loss of aroma, colour, texture and flavor [15,55]. On the other hand, IR drying is considered a promising method of food dehydration in which IR electromagnetic radiation impinges on the exposed material and is absorbed at the surface based on the absorptivity of the material [18,49]. IR increases the moist material temperature and evaporates its moisture by action of infrared wavelength radiation from a source that interacts with the internal structure of the product [56]. It is energy efficient, environmentally friendly and characterized by the homogeneity of heating, a high transfer rate, a low drying time, low energy consumption, a higher degree of process control and improved product quality and food safety [15,57]. The use of infrared heating for food and ornamental plant drying keeps growing [15,57,58]. Particularly, for apple drying, few published works have addressed the use of IR in comparison to other drying methods such as OV [14,15,59,60]. However, continuous studies on apples drying under various drying conditions are needed for process optimization and to advance the literature knowledge. Usually, the standard hot air oven drying method is not equipped with an in-built data acquisition software. Monitoring the sample weight manually affects the drying process. The drying process enables determination of moisture content of a given sample by evaporating its free water and other components. The sample's moisture content is determined by means of precise weighing carried out before and during the process [58]. The current research provides information on the data acquisition on the hot air oven drying process in comparison with the infrared drying process with the data collection function. Therefore, this present study aimed to investigate the drying kinetics, colour measurements and mathematical modeling of red delicious apple slices under infrared (IR) and hot air oven (OV) drying methods at different drying temperatures at a constant drying time of 10 h. The results were compared with published studies on the thin-layer drying of different apple varieties under hot air oven and infrared drying methods.

2. Materials and Methods

2.1. Sample and Drying Methods

Fresh whole red delicious apples (Figure 1a) were purchased from a supermarket in Prague, Czech Republic. The samples were stored in the refrigerator at 5 °C. Before the experiments, the samples were removed and allowed to cool to a laboratory temperature of 24.26 ± 0.50 °C and humidity of 41.6 ± 2.42%. A slicer was used to cut the fresh apples into a cylindrical size of thickness of 8.07 ± 0.05 mm and diameter of 66.27 ± 3.13 mm. The dimensions (diameter and thickness) of the fresh and dried apple sliced samples were accurately measured using a digital calliper with an accuracy of 0.01 mm. The mass of the fresh and dried apple sliced samples was measured using a digital balance with an accuracy of 0.01. Infrared and hot air oven equipment was used to dry the freshly sliced apple samples (Figure 1b–d) at different drying temperatures from 40 °C to 80 °C with 10 °C intervals. The standard hot air oven (MEMMERT UF55m GmbH + Co. KG, Buechenbach, Germany) using hot air and the moisture analyser Radwag MA 50/1.R (Warsaw, Poland) were used for the drying experiments of the freshly sliced apple samples. For the hot air oven drying equipment, custom measuring equipment based on Radaxa Rock Pi 4 was used. Samples of weight measurement between 0 and 100 g sensor via HX711 AD converter (AVIA, Shenzhen, China) with a software temperature compensation was used for the weight data recording, and a digital sensor DS18B20 (Maxim Integrated Products GmbH, Landsberger, Munich, Germany) was used for the temperature monitoring inside

the hot air oven. The moisture analyser is designed to test moisture content by heating the samples, which is done using an infrared (IR) emitter, a halogen or a metal heater [58]. The weighing pan dimensions are 90 mm diameter and 8 mm height. The maximum sample weight and height of the equipment are 50 g and 20 mm. The maximum drying temperature range is 160 °C. The power consumption is 4 W and heating module power is 450 W. The drying method was set on the fast mode. The drying equipment is programmed for the temperature, time and time interval for the weight measurement during the drying process. The drying process completes automatically for the given time setting and the data are stored.

2.2. Colour Analysis

The colour values of the fresh and dried apple slices at the different drying temperatures were measured using the RGB colour analyser Voltcraft Plus RGB-2000 (Voltcraft, Lindenweg 15, D-92242 Hirschau, Germany). The RGB (red, green and blue) values were converted to lab values using an online converter. The total colour change (ΔE), chroma (ΔC), colour index (*CI*), whiteness index (*WI*), browning index (*BI*) and hue angle (*Hue°*) of the fresh and dried sliced apples under different drying temperatures for both infrared and hot air oven methods were calculated using Equations (1) to (10) [11,16,20,23,27,28,35,48,51,57,61–66].

$$\Delta E = \sqrt{\left(L_O^* - L^*\right)^2 + \left(a_O^* - a^*\right)^2 + \left(b_O^* - b^*\right)^2} \tag{1}$$

$$\Delta C = \sqrt{\left(a_O^* - a^*\right)^2 + \left(b_O^* - b^*\right)^2} \tag{2}$$

$$CI = \frac{1000 \cdot a^*}{L^* \cdot b^*} \tag{3}$$

$$WI = 100 - \sqrt{\left(100 - L^*\right)^2 + a^{*2} + b^{*2}} \tag{4}$$

$$BI = \frac{[100(x - 0.31)]}{0.17} \tag{5}$$

$$x = \frac{\left(a^* + 1.75 \cdot L^*\right)}{\left(5.645 \cdot L^* + a^* - 3.012 \cdot b^*\right)} \tag{6}$$

$$Hue° = tan^{-1}\left(\frac{b^*}{a^*}\right) \tag{7}$$

(when $a^* > 0$ and $b^* \geq 0; 0° < Hue < 90°$)

$$Hue° = 180 + tan^{-1}\left(\frac{b^*}{a^*}\right) \tag{8}$$

(when $a^* < 0$ and $b^* \geq 0; 90° < Hue < 180°$)

$$Hue° = 180 + tan^{-1}\left(\frac{b^*}{a^*}\right) \tag{9}$$

(when $a^* < 0$ and $b^* < 0; 180° < Hue < 270°$)

$$Hue° = 360 + tan^{-1}\left(\frac{b^*}{a^*}\right) \tag{10}$$

(If $a^* > 0$ and $b^* < 0; 270° < Hue < 360°$)

where L_O^*, a_O^* and b_O^* represent the fresh samples, whereas L^*, a^* and b^* represent the dried samples. The L^* colour parameter is in a range from 0 (blackness) to 100 (whiteness). The a^* parameter is from $-a^*$ (greenness) to $+a^*$ (redness) and the b^* parameter is from $-b^*$ (blueness) to $+b^*$ (yellowness). The chroma (C) indicates the colour's saturation or purity [11,16,61,67].
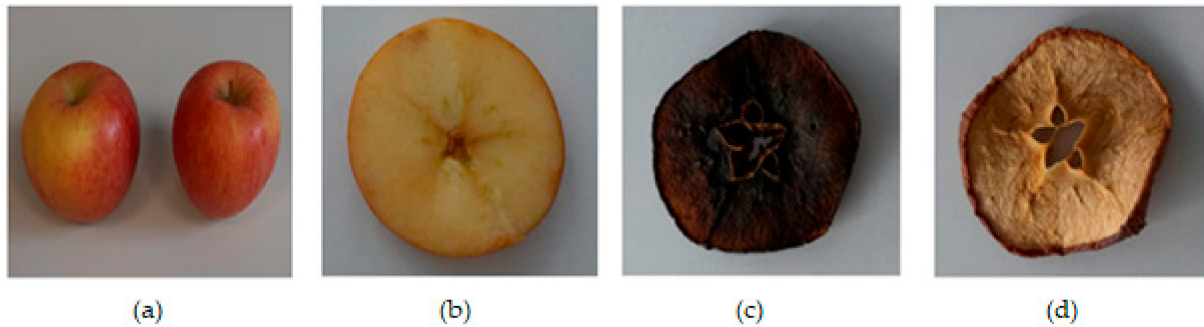
Figure 1. Two fresh samples of whole red delicious apples (**a**), freshly sliced sample (**b**), infrared dried sliced sample (**c**) and hot air oven-dried sliced sample (**d**) at a drying temperature of 80 °C [61].

2.3. Dry Basis Moisture Content

The dry basis moisture content M_t of the samples was calculated using Equation (11) [18,66,68].

$$M_t = \frac{(W_t - G)}{G} \tag{11}$$

where M_t is the dry basis moisture content of the sample at the moment of drying time t, (g/g); W_t is the total mass of sample (g) at the moment of drying time t and G is the mass of dry matter (g).

2.4. Moisture Ratio

The moisture ratio MR was calculated using Equation (12) [66,68,69].

$$MR = \frac{M_t}{M_o} \tag{12}$$

where M_o is the initial dry-basis moisture content (g/g).

2.5. Rehydration Ratio

The rehydration ratio RR (g/g) was carried out according to the published procedure [62,65,66,70]. Following the procedure, the weighted dehydrated samples were dipped into a beaker of hot water at 80 °C for 15 min. The rehydrated samples were filtered over a screen for 2 min and thereafter were blotted with an absorbent paper and then weighted again. The RR of the dried samples was calculated using Equation (13).

$$RR = \frac{W_{rs}}{W_{ds}} \tag{13}$$

where W_{rs} is the weight of the rehydrated sample (g) and W_{ds} is the weight of the dried sample (g). The rehydration capacity measures the physical and chemical changes that occur in the product during the drying process [16].

2.6. Shrinkage

In a drying process, the shrinkage *SK* (%) refers to the volume reduction or the change in selected dimensions due to the moisture removal from the sample structure [31,62,66,67]. The shrinkage of the samples was calculated using Equations (14) to (16) [71,72].

$$SK = \left[\frac{V_O - V_f}{V_O}\right] \times 100 \tag{14}$$

where V_O is the initial volume of the fresh sample (mL) and V_f is the final volume of the dried sample (mL).

$$V_O = \pi\left(\frac{D_O}{2}\right)^2 \cdot t_O \tag{15}$$

$$V_f = \pi\left(\frac{D_f}{2}\right)^2 \cdot t_f \tag{16}$$

where D_O and D_f and t_O and t_f are the initial and final diameters (mm) and thicknesses (mm) of the sample.

2.7. Bulk Density

The bulk density (g/mL) of the dried samples was calculated using Equation (17) [62,66,73].

$$\rho_{bulk} = \frac{m}{V} \tag{17}$$

where *m* is the weight of the dried sample (g) and *V* is the volume of the dried sample (mL).

2.8. Surface Area

The surface area *A* (mm^2) of the fresh and dried sliced samples was calculated using Equation (18) [17,66].

$$A = 2\pi r(r + h) \tag{18}$$

where *r* is the radius (mm) and *h* is the thickness (mm) of the fresh and dried samples.

2.9. Applied Mathematical Models to the Drying Curves

The mathematical models applied to the drying curves of dried apple sliced samples under infrared and hot air oven drying temperatures and methods are given in Table 1.

Table 1. Selected thin layer mathematical models for drying curves description.

Model Name	Model	References
Newton and Lewis	$MR = \exp(-k \cdot t)$	[20,45,67,74,75]
Page	$MR = \exp(-k \cdot t^n)$	[20,45,67,74–76]
Modified page	$MR = \exp\left[-(k \cdot t)^n\right]$	[45,75,77]
Henderson and Pabis	$MR = a \cdot \exp(-k \cdot t)$	[45,75,78]
Logarithmic	$MR = a \cdot \exp(-k \cdot t) + c$	[20,45,67,75,79]
Two-term	$MR = a \cdot \exp(-k_o \cdot t) + b \cdot \exp(-k_1 \cdot t)$	[20,45,75,80]
Two-term exponential	$MR = a \cdot \exp(-k \cdot t) + (1 - a)\exp(-k \cdot a \cdot t)$	[45,67,75,77]
Wang and Singh	$MR = 1 + a \cdot t + b \cdot t^2$	[45,67,75,81]
Approximation of diffusion	$MR = a \cdot \exp(-kt) + (1 - a)\exp(-k \cdot b \cdot t)$	[20,45,67,75,79]
Verma et al., 1985 [82]	$MR = a \cdot \exp(-k \cdot t) + (1 - a)\exp(-g \cdot t)$	[20,45,67,82]
Modified Henderson and Pabis	$MR = a \cdot \exp(-k \cdot t) + b \cdot \exp(-g \cdot t) + c \cdot \exp(-h \cdot t)$	[45,75,83]
Midilli et al., 2002 [84]	$MR = a \cdot \exp(-k \cdot t^n) + b \cdot t$	[20,45,67,84]
Weibull distribution	$MR = a - b \cdot \exp(-(k \cdot t^n))$	[21,85]
Alibas	$MR = a \cdot \exp((-k \cdot t^n)) + (b \cdot t)) + g$	[21,86]

MR: moisture ratio; *n*: number of constants in the model; *k*, k_o, k_1, *g* and *h*: drying constants and *a*, *b* and *c*: coefficients and *t*: drying time (min).

2.10. Models Fitting of Experimental Drying Curves

The experimental drying curves of the sliced apple samples at different drying temperatures under infrared and hot air oven methods (Figure 2) were fitted based on the thin-layer mathematical models described in Table 1. The function curve fit from the Python library scipy.optimize was used to generate the coefficients of the models.
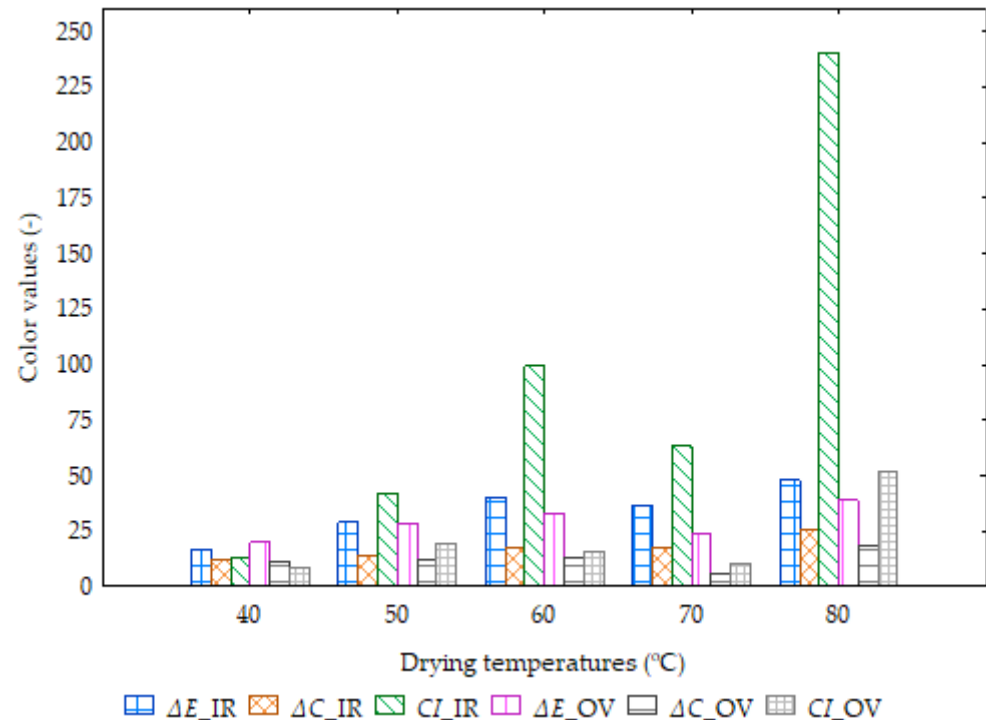
Figure 2. Column plots of colour values (total colour difference (ΔE), chroma (ΔC), and colour index (CI)) of dried apple sliced samples under infrared (IR) and hot air oven (OV) drying temperatures.

2.11. Validation Metrics for Fitted Mathematical Models

The root mean square error (RMSE), reduced chi-square (χ^2), coefficient of determination (R^2) and modelling efficiency (EF) as described in Equations (19) to (22) were used to evaluate the suitability of the thin-layer mathematical models for describing the obtained drying curves [23,25,27,44,45,77,87,88]. The RMSE gives the deviation between the predicted and experimental values, and it is preferred to tend to zero. The reduced chi-square is the mean square of the deviations between the experimental and predicted values of the models which measures the goodness of fit. The R^2 and the EF also measure the ability of the model to predict the drying behaviour of the product and its highest value is one.

$$RMSE = \sqrt{\frac{\sum_{i=1}^{N}\left(MR_{pre,\,i} - MR_{exp,\,i}\right)^2}{N-n}} \tag{19}$$

$$X^2 = \frac{\sum_{i=1}^{n}\left(MR_{pre,\,i} - MR_{exp,\,i}\right)^2}{N-n} \tag{20}$$

$$R^2 = \frac{\sum_{i=1}^{N}\left(MR_i - MR_{pre,\,i}\right)\left(MR_i - MR_{exp,\,i}\right)}{\sqrt{\left[\sum_{i=1}^{N}\left(MR_i - MR_{pre,\,i}\right)^2\right]\left[\sum_{i=1}^{N}\left(MR_i - MR_{exp,\,i}\right)^2\right]}} \tag{21}$$

$$EF = \frac{\sum_{i=1}^{n}(MR_{i,exp} - MR_{i,exp_{mean}})^2 - \sum_{i=1}^{n}(MR_{i,pre} - MR_{i,exp})^2}{\sum_{i=1}^{n}(MR_{i,exp} - MR_{i,exp_{mean}})^2} \qquad (22)$$

where $MR_{exp, i}$ is the measured moisture ratio, $MR_{pre, i}$ is the predicted moisture ratio, N is the number of observations and n is the number of constants in the drying model.

2.12. Statistical Analyses

The experiments were repeated twice and the data were presented as the means, standard deviation and percentage coefficient of variation. The data were also subjected to correlation and single-factor ANOVA analyses at a 95% confidence interval using Statistica software, version 13 [89].

3. Results and Discussion

3.1. Calculated Parameters under Drying Temperatures and Methods

The mean, standard deviation and percentage coefficient of variation of the calculated parameters of fresh and dried sliced apple samples under the infrared (IR) and hot air oven (OV) drying methods at drying temperatures of 70 °C and 80 °C are given in Tables 2 and 3. The results of the drying temperatures between 60 and 40 °C are also provided in the Supplementary Material (Tables S1–S3). Lower values of the standard deviation to the mean or lower percentage coefficient of variation are based on the assumption that observations follow normal or symmetrical statistical distribution [90,91]. The graphical descriptions of the calculated parameters are shown in Figures 2–4 and the Supplementary Material (Figures S1 and S2).

Table 2. Calculated parameters of sliced apple samples at drying temperatures of 70 °C using infrared and hot air oven drying methods.

Calculated Parameters	Infrared Drying at 70 °C			Hot Air Oven Drying at 70 °C		
	Mean	**±SD**	**% CV**	**Mean**	**±SD**	**% CV**
L_O^*	42.883	3.902	9.099	43.984	1.643	3.736
L^*	11.097	6.857	61.793	20.716	5.291	25.539
a_O^*	6.244	0.721	11.551	7.392	0.904	12.236
a^*	7.350	6.515	88.640	5.458	1.328	24.330
b_O^*	29.012	0.793	2.735	24.055	7.200	29.934
b^*	12.536	10.776	85.961	25.083	0.603	2.405
ΔE	36.773	7.520	20.449	24.085	3.370	13.990
ΔC	17.676	10.332	58.451	6.128	0.605	9.873
CI	63.254	36.841	58.244	10.525	0.384	3.650
WI	9.409	4.710	50.052	16.642	4.764	28.642
BI	275.138	156.695	56.951	417.610	243.270	58.253
$Hue°$	60.081	1.072	1.785	77.768	2.611	3.357
RR	1.670	0.144	8.637	2.053	0.027	1.332
SK	53.722	0.469	0.873	56.790	1.425	2.508
ρ_{bulk}	0.284	0.027	9.360	0.315	0.022	7.008
A_O	9005.683	730.973	8.117	9368.521	145.169	1.550
A_f	5825.287	436.630	7.495	6602.650	165.364	2.505
V_O	30.923	1.714	5.542	31.021	0.736	2.372
V_f	14.307	0.648	4.531	13.399	0.124	0.927

CV: Coefficient of variation; ±SD: Standard deviation; L_O^*, a_O^* and b_O^* represent fresh samples and L^*, a^* and b^* represent dried samples as lightness, greenness/redness and blueness/yellowness; total colour difference (ΔE), chroma (ΔC), colour index (CI), whiteness index (WI), browning index (BI); hue angle ($Hue°$); rehydration ratio RR (g/g); shrinkage SK (%) and bulk density ρ_{bulk} (g/mL); A_O: initial area of the fresh sample (mm²); A_f: final area of the dried sample (mm²); V_O is the initial volume of the fresh sample (mL); V_f is the final volume of the dried sample (mL).

Table 3. Calculated parameters of sliced apple samples at drying temperatures of 80 °C using infrared and hot air oven drying methods.

Calculated Parameters	Infrared Drying at 80 °C			Hot Air Oven Drying at 80 °C		
	Mean	**±SD**	**% CV**	**Mean**	**±SD**	**% CV**
L_O^*	43.223	2.933	6.786	46.425	3.258	7.017
L^*	3.088	1.165	37.737	12.188	10.316	84.644
a_O^*	4.601	1.360	29.557	4.502	2.672	59.361
a^*	0.679	0.431	63.468	4.181	3.416	81.713
b_O^*	26.719	0.169	0.633	28.923	1.838	6.354
b^*	1.026	0.711	69.297	10.806	9.276	85.840
ΔE	47.844	1.046	2.185	38.810	9.705	25.006
ΔC	26.018	0.805	3.093	18.125	7.447	41.089
CI	240.154	107.063	44.581	52.216	46.272	88.616
WI	3.078	1.155	37.509	11.074	8.899	80.357
BI	52.496	20.608	39.257	186.910	4.467	2.390
$Hue°$	55.838	1.990	3.565	68.317	1.250	1.830
RR	1.699	0.117	6.893	1.670	0.234	13.991
SK	39.815	2.671	6.708	57.282	4.745	8.283
ρ_{bulk}	0.187	0.008	4.088	0.338	0.009	2.666
A_O	9055.354	1001.409	11.059	8245.719	970.837	11.774
A_f	8795.898	1003.753	11.412	7625.466	828.761	10.868
V_O	29.719	4.558	15.337	27.149	3.794	13.976
V_f	17.826	1.950	10.937	11.507	0.334	2.898

CV: Coefficient of variation; ±SD: Standard deviation; L_O^*, a_O^* and b_O^* represent fresh samples and L^*, a^* and b^* represent dried samples as lightness, greenness/redness and blueness/yellowness; total colour difference (ΔE), chroma (ΔC), colour index (CI), whiteness index (WI), browning index (BI); hue angle ($Hue°$); rehydration ratio RR (g/g); shrinkage SK (%) and bulk density ρ_{bulk} (g/mL); A_O: initial area of the fresh sample (mm²); A_f: final area of the dried sample (mm²); V_O is the initial volume of the fresh sample (mL); V_f is the final volume of the dried sample (mL).

Figure 3. Column plots of colour values (whiteness index (*WI*), browning index (*BI*) and hue angle (*Hue°*)) of dried apple sliced samples under infrared (IR) and hot air oven (OV) drying temperatures.
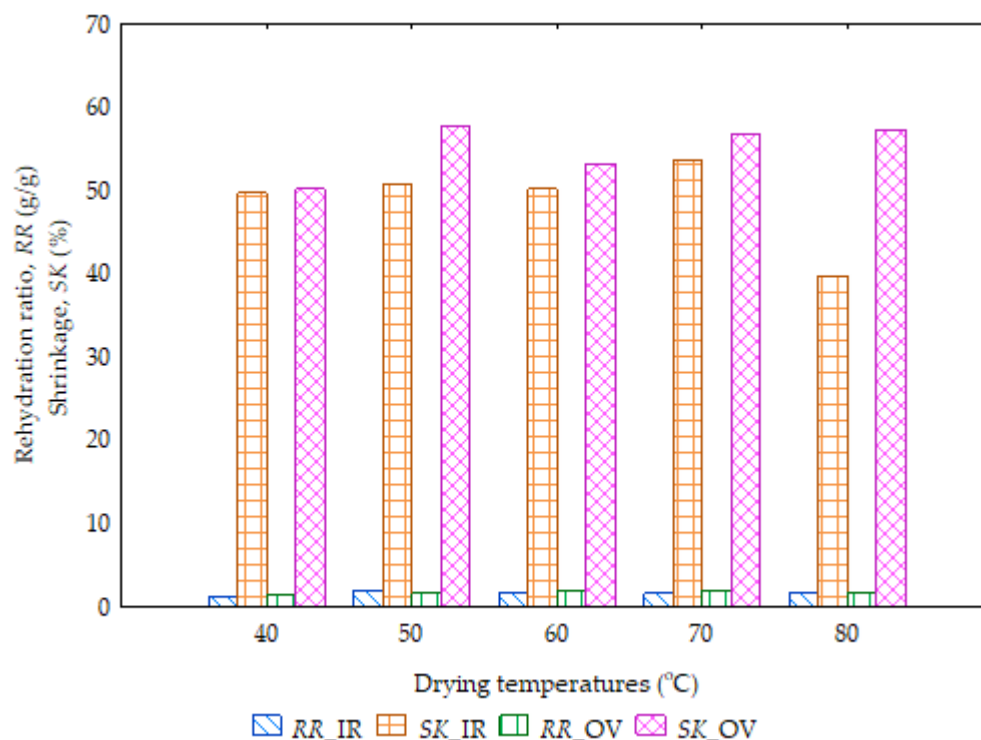
Figure 4. Column plots of rehydration ratio (g/g) and shrinkage *SK* (%) of dried apple sliced samples under infrared (IR) and hot air oven (OV) drying temperatures.

3.2. Evaluation of Colour Parameters

Colour is one of the major quality attributes that specify the quality of the final product and thus influences consumer preference. When samples of fruits and vegetables are subjected to heat treatments non-enzymatic browning and pigment destruction can cause colour changes [11,16,26,28,65]. Cruz et al. [92] as cited in Ghinea et al. [48] stated that the change in colour during drying is associated with the development of browning reactions which are attributed to the activity of the enzyme polyphenol oxidase. In this study, the general observation was that the values of the calculated colour parameters for fresh samples: L_O^*, a_O^* and b_O^* and dried samples: L^*, a^* and b^* representing the lightness, greenness/redness and blueness/yellowness increased and decreased along with the drying temperatures between 40 and 80 °C for both infrared (IR) and hot air oven (OV) drying methods. Mostly, lower values were observed at 80 °C for IR compared to OV which showed higher values. The total colour change (ΔE), chroma (ΔC), colour index (*CI*), whiteness index (*WI*) and browning index (*BI*) showed both increasing and decreasing trends with the drying temperatures for IR and OV drying methods. For the drying temperatures between 60 °C and 80 °C, all the colour indicators were lower under IR method compared to OV method which showed higher values. However, for the drying temperatures of 40 °C and 50 °C, all the colour indicators were higher under IR method compared to OV method which produced lower values.

In comparison with other published studies, for instance, Izli et al. [28] found that the colour parameters of L^* and b^* of dried samples of kumquat slices decreased with an increase in drying temperatures between 50 °C and 80 °C, whereas a^* values showed an increment with an increase in drying temperatures. Again, Izli et al. [28] under the same processing conditions reported a total colour change (ΔE) of dried kumquat slices ranging from 14.82 to 30.52. In this study, however, the ΔE values ranged from 19.76 ± 16.07 to 38.10 ± 9.71 uder OV. High values of ΔE were observed at high drying temperatures which were in agreement with the result of Lechtanska et al. [93], who reported the total colour change of dried green pepper in a range between 9.41 ± 0.33 and 13.30 ± 0.34. The authors [93] mentioned that the intensity of green pepper colour change depended

mainly on the duration of its exposure to high temperatures during drying. Bozkir and Ergun [62] also reported similar values for dried persimmon fruits with ultrasound and osmotic dehydration pretreatments using hot air drying. Chroma (ΔC) values indicate the purity of colour as reported by Izli et al. [28]. The authors [28] found a decreasing trend of chroma values with an increase in drying temperatures for dried kumquat slices, indicating its colour instability. The hue angle values of the dried apple sliced samples for OV were higher than the IR at all drying temperatures. The values ranged from 48.66 ± 7.26 to $81.48 \pm 1.77°$. The hue angle is a parameter that is commonly used for the characterization of colour in edible products [11]. Bozkir and Ergun [62] reported hue angle values between 32.72 ± 0.19 and $34.31 \pm 0.96°$ for dried persimmon fruits. Jafari et al. [11] also reported hue angle values between 76.11 and 89.99° for fresh and dried eggplant slices under infrared drying. The authors observed that the hue angle values decreased within the drying processes (slice thicknesses, air velocities and infrared powers) where the decrease implied a decrease from a green-yellow with a hue angle of $\cong 90°$ to a yellow-orange with a hue angle < 90 °. Izli et al. [28] reported similar observations of chroma values for hue angle values. The authors indicated that the reduction in hue angle values of dried samples of kumquat slices is an expression of more browning than yellowness. The browning index values under IR and OV drying methods did not show a linear function with the drying temperatures. However, in a convective hot air dryer study by Sacilik and Elicin [13] as cited in Izli et al. [28], it was indicated that the browning of dried organic apple slices increased with increasing drying temperatures which was in agreement with the study by Ghinea et al. [48]. The whiteness index (*WI*) corresponds to the product discolouration and lesser browning [64,65,94]. It was observed that *WI* values of the dried apple slices under the IR were lower than OV for all drying temperatures except at 40 °C which was the opposite. The study by Ghinea et al. [48] also showed that *WI* values of different varieties of dried apple slices differed among the two drying methods (oven and dehydrator). The column plots of the colour parameters of dried apple sliced samples under IR and OV drying temperatures are illustrated in Figures 2 and 3.

3.3. Rehydration Ratio and Shrinkage

The rehydration ratio values increased linearly at drying temperatures from 40 °C to 70 °C but decreased at 80 °C for OV. However, for IR, the values increased from 40 °C to 50 °C but decreased from 50 °C to 70 °C with a slight increase at 80 °C. The values ranged from 1.33 ± 0.29 to 2.05 ± 0.03. Similar results were reported by Aral and Bese [16], Bozkir et al. [22] and Bozkir and Ergun [62] for dried hawthorn fruit under different drying temperatures between 50 and 70 °C and air velocities between 0.5 and 1.3 m/s and dried persimmon fruit samples under ultrasound and osmotic dehydration pre-treatments with hot air drying. Aral and Bese [16] found that the rehydration ratio of dried samples at higher drying temperatures was higher than those dried at lower drying temperatures. The explanation was that dried samples at higher temperatures have a more porous structure than dried samples at lower temperatures and this porosity allows the higher water [16]. The rehydration ratio of dried samples is dependent on the extent of the structural damage during drying [95]. A higher rehydration ratio leads to a smaller degree of structural damage to the dried product with a better quality [49]. Baysal et al. [96] reported a higher rehydration capacity of infrared-dried carrots as compared to that dried using hot air or microwave, as cited in [97]. Vishwanathan et al. [97] in a separate study reported uniform and rapid heating by infrared radiation and the absence of case hardening was responsible for a greater degree of rehydration. The authors [97] further indicated that rapid heating with infrared and quicker diffusion of water vapour within the material could facilitate the sample to retain its porous structure, thereby increasing its ability to absorb a higher amount of water during rehydration.

Shrinkage values showed both increasing and decreasing trends for OV and IR methods along with the drying temperatures. A lower value of $39.82 \pm 2.67\%$ was observed at 80 °C for IR compared to the OV, where a higher value of $57.28 \pm 4.75\%$ was observed.

However, the highest shrinkage value of 57.80 ± 0.47% was observed for OV at 50 °C. There was no direct effect of the drying temperatures on the shrinkage of dried apple sliced samples under OV and IR. Sturm et al. [51] indicated that the degree of shrinkage depends directly on the temperature, humidity and velocity levels applied. The authors [51] further explained that when air temperature is kept constant, shrinkage is significantly higher than the specimen which is initially dried at very high air temperatures. This is because slow drying reduces internal stresses which consequently results in increased shrinkage. However, applying high temperatures increases internal stresses but at the same time, the resulting fast drying leads to a mechanical stabilization of the surface [51,98,99]. Furthermore, Aral and Bese [16] reported that the shrinkage of dried hawthorn fruit increased with decreasing drying temperature, which was attributed to the slow drying rate at low temperatures and moisture distribution which was uniform in the fruit. Furthermore, the authors [16] stated that at higher temperatures, the drying rate is high and leads to a mechanical stabilization of the surface which limits the degree of shrinkage. Dhurve et al. [100] indicated that the shrinkage of dried watermelon seeds using a convective dryer increased with increased drying temperature. The column plots of the rehydration ratio and shrinkage of the dried apple sliced sample at different drying temperatures for OV and IR are displayed in Figure 4.

3.4. Bulk Density, Final Area and Final Volume

The bulk density of the dried apple sliced samples using OV decreased from 40 °C to 70 °C with a slight increase at 80 °C. However, compared to the IR, the values decreased from 40 °C to 50 °C and then at 80 °C but a linear increase was observed from 50 °C to 70 °C. The values ranged from 0.19 ± 0.01 to 0.46 ± 0.04 g/mL. Bozkir et al. [22] and Bozkir and Ergun [62] also reported bulk density values between 0.891 ± 0.018 to 1.006 ± 0.015 g/mL for dried persimmon fruit samples. The final area of the dried apple sliced samples for the OV method at the different drying temperatures linearly increased compared to the IR, where a slight linear trend was observed between 60 °C and 80 °C. The values of the final area of the dried apple sliced samples for OV ranged from 5707.06 ± 1528.09 to 7625.47 ± 828.76 mm^2 whereas the IR values ranged from 5162.86 ± 502.05 to 8795.89 ± 1003.75 mm^2. The final volume also increased from 50 to 70 °C but then decreased at 80 °C for OV whereas a slight increase was observed for IR from 60 to 80 °C with a decrease observed from 50 to 60 °C. The volume values ranged from 11.51 ± 0.33 to 17.83 ± 1.95 mL. Cetin et al. [17] reported the final area values between 1391.21 and 2767.67 mm^2 and final volume values between 4184.06 and 6611.78 mm^3 for Red Chief variety apple at different drying conditions (slice thicknesses of 5 and 7 mm, drying times of 9 and 10 h and heating temperatures of 50 and 60 °C).

3.5. Experimental Drying Curves

The experimental drying curves are described in Figure 5a–d. The drying curves showed that the drying temperature influenced drying rates. At all drying temperatures, higher moisture removal was observed for IR compared to the OV. For both IR and OV drying methods, the drying time of 10 h was not enough to dry the sliced apple sample at 40 °C to reach the equilibrium sample weight or moisture content. The equilibrium moisture content was reached for the drying temperatures from 50 °C to 80 °C (Figure 5a,b). The observed moisture content values were below 6 g/g dry basis. According to Wang et al. [49], Murugesan et al. [101] and Yu et al. [102], during the drying process, the moisture transportation from the material to the drying medium is driven by the moisture concentration difference between the drying medium and the material surface, and the total drying time is predominantly governed by the relative humidity of the drying medium. The authors further stated that a lower relative humidity of the drying medium results in a shorter drying time. The obtained drying curves were in agreement with some published studies on the drying of various agricultural products [18,23,25,37,43,57,94,103–109].
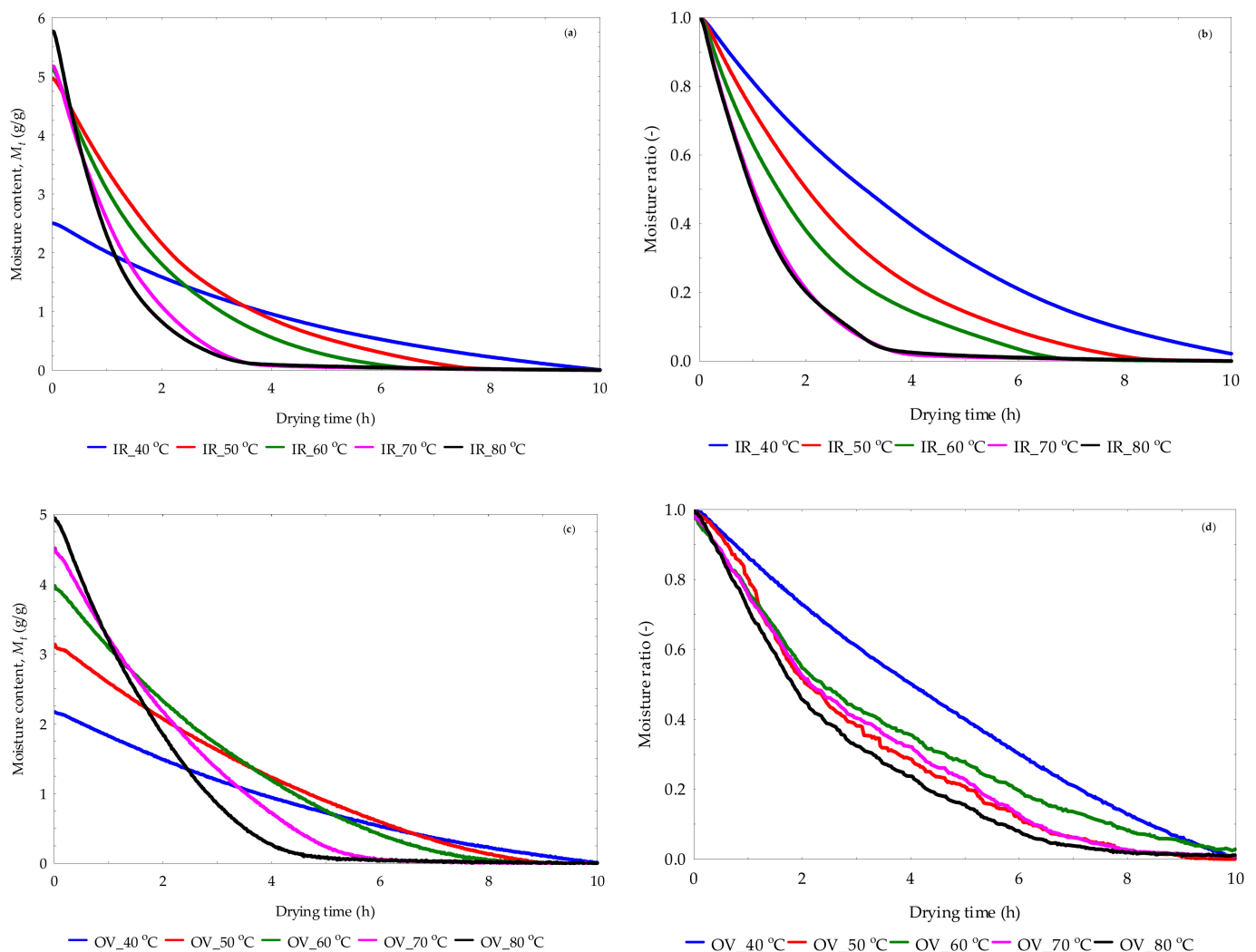
Figure 5. (**a**) Dry basis moisture content and (**b**) moisture ratio versus drying time curves under infrared (IR) and (**c**) dry basis moisture content and (**d**) moisture ratio versus drying time curves under hot air oven (OV) at different drying temperatures of dried apple sliced samples.

3.6. Model Fitting of Drying Curves and Validation Metrics

From the drying curves thin layer mathematical models mentioned in Table 1, the page, logarithmic and Weibull distribution models best described the experimental drying curves of the dried apple sliced samples at the drying temperatures between 40 and 80 °C under infrared and hot air oven drying methods. The models' coefficients/constants at 70 and 80 °C for describing the drying curves are presented in Table 4a–c. The estimated values for the drying temperatures between 60 and 40 °C are also presented in the Supplementary Material (Table S4a–c). The Weibull distribution model was found most suitable for describing the drying processes of dried apple slices at different drying temperatures (Figure 6). The goodness of fit of the drying models was assessed by the root mean square error (RMSE), chi-square (χ^2), coefficient of determination (R^2) and modelling efficiency (EF). The smaller the RMSE and χ^2 values and the greater the R^2 and EF values the better the goodness of fit of the model to the experimental drying curves [16,45,67,103,104,108,110]. Aral and Bese [16] fitted their experimental data on the thin layer hawthorn fruit under convective drying with eleven different mathematical models. The authors indicated that Midilli et al.'s [84] model was the most appropriate for explaining the drying behaviour of hawthorn fruit sliced samples. Similar results were found by Meisami-asl et al. [45] on thin layer drying kinetics of apple slices

(variety Golab) at different temperatures between 40 and 80, velocities at 0.5 m/s and thickness of thin layer between 2 and 6 mm; Menges and Ertekin [44] on golden apples at drying air temperatures of 60, 70 and 80 and velocities of 1.0, 2.0 and 3.0 m/s and Aradwad et al. [15] on apple slices under the influence of infrared power wattage and hot air drying temperatures. Furthermore, Karaaslan et al. [19] found the Weibull distribution as the best descriptive model for all the drying experiments of thin layer grape fruit samples under the different drying methods except for the combined microwave and convective drying where the Alibas model was the best descriptive model. Blanco-Cano et al. [30] found that Wang–Singh equation precisely described the drying process of Granny Smith sliced apples at variable drying temperatures.

Table 4. (**a**) Fitting parameter values and statistical validation metrics for drying sliced apple samples at 70 °C and 80 °C drying temperatures using infrared, IR and hot air oven, OV drying methods. (**b**) Weibull distribution model fitting parameter values for drying sliced apple samples at 70 °C and 80 °C drying temperatures using infrared, IR and oven, OV drying methods. (**c**) Statistical validation metrics for the Weibull distribution model.

(a)

Model Name	T_p (°C)	Drying Methods	Model Coefficients/Constants (k, n, a, and c)			RMSE	χ^2	R^2	EF
Page *	70 **	IR *	k 0.005487	n 1.189299		0.070680	0.000041	0.999248	0.999992
		OV *	0.001358	1.320076		0.124774	0.000338	0.996488	0.99909
Logarithmic *	70 **	IR *	a 1.077076	k 0.013660	c −0.005972	0.104138	0.000190	0.996488	1
		OV *	1.123411	0.006597	−0.057317	0.150237	0.000680	0.991783	1
Page *	80 **	IR *	k 0.010195	n 1.101400		0.063898	0.000024	0.999653	0.999259
		OV *	0.001911	1.315627		0.094260	0.000146	0.998141	0.999737
Logarithmic *	80 **	IR *	a 1.053957	k 0.016772	c 0.001478	0.063429	0.000035	0.999205	1
		OV *	1.113527	0.009167	−0.025581	0.145513	0.000625	0.991444	1

(b)

Model Name	T_p (°C)	Drying Methods	Model Coefficients/Constants			
			k	a	b	n
Weibull distribution	70 **	IR *	0.004899	0.001273	−0.98763	1.212419
		OV *	0.000938	−0.01397	−0.96946	1.37482
	80 **	IR *	0.010951	0.004149	−1.01219	1.091566
		OV *	0.001302	−0.00257	−0.96673	1.38421

(c)

Model Name	T_p (°C)	Drying Methods	Statistical Metrics			
			RMSE	χ^2	R^2	EF
Weibull distribution	70 **	IR *	0.067883	0.000039	0.999284	1
		OV *	0.108892	0.000188	0.997744	1
	80 **	IR *	0.050042	0.000009	0.999806	1
		OV *	0.090309	0.000105	0.998569	1

*: See model description in Table 1; **: Experiment 2 dataset; T_p: Drying temperature; RMSE: Root mean square error; χ^2: chi-square; R^2: Coefficient of determination and EF: Modelling efficiency.
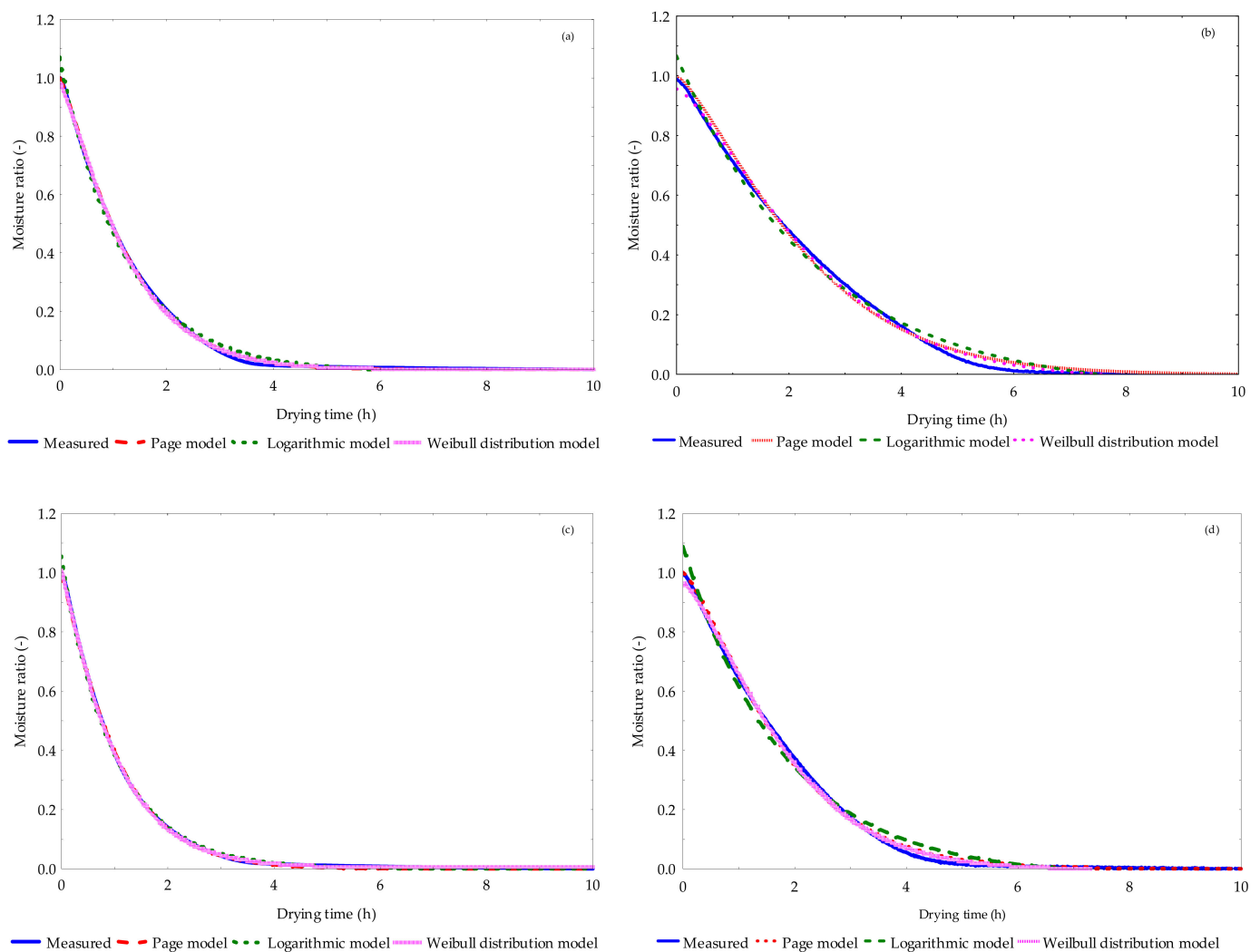
Figure 6. Measured and fitted curves of dried apple sliced samples under (**a**) infrared and (**b**) hot air oven drying at 70 °C and (**c**) infrared and (**d**) hot air oven drying at 80 °C.

3.7. Evaluation of Linear Correlation and ANOVA Analyses

The correlation results for the calculated parameters versus the drying temperature of the sliced apple samples dried under infrared and hot air oven drying methods are provided in Table 5. All the calculated parameters correlated both positively and negatively under both drying methods. However, under the infrared drying, only the lightness L^*, greenness/redness b^* of the dried sample, total colour difference (ΔE), chroma (ΔC), colour index (*CI*), whiteness index (*WI*), bulk density ρ_{bulk} (g/mL), final area of the dried sample A_f and the final volume of the dried sample V_f were significantly affected (*p*-value < 0.05) by the drying temperature. This means that whereas the total colour parameters increased along with the drying temperature, the whiteness index and the bulk density decreased. Regarding the hot air oven drying, all the calculated parameters were not significantly affected (*p*-value > 0.05) by the drying temperature except the bulk density and the final area of the sample which showed significance. The summary of the ANOVA analysis is shown in Table 6. The ANOVA results revealed that for all the calculated parameters, only the lightness of the dried sample L^*, total colour difference (ΔE), colour index (*CI*), whiteness index (*WI*), bulk density ρ_{bulk} (g/mL), final area of the dried sample A_f (mm^2) and the final volume of the dried sample V_f (mL) were significant (*p*-value < 0.05) against the effect of the drying temperature. In comparison with the hot air oven drying method, only the hue angle, bulk density and rehydration capacity were statistically significant

(p-value < 0.05). The detailed ANOVA univariate results of the significant parameters are presented in the Supplementary Material (Tables S5 and S6), respectively.

Table 5. Correlation results of the effect of infrared and hot air oven drying temperatures for drying sliced apple samples.

Calculated Parameters	Infrared Drying Temperature °C		Hot Air Oven Drying Temperature °C	
	Correlation Coefficient, r	p-Value	Correlation Coefficient, r	p-Value
L_O^*	0.380	>0.05	0.419	>0.05
L^*	−0.847	<0.05	−0.281	>0.05
a_O^*	−0.316	>0.05	−0.013	>0.05
a^*	−0.620	>0.05	0.156	>0.05
b_O^*	−0.216	>0.05	0.076	>0.05
b^*	−0.799	<0.05	−0.097	>0.05
ΔE	0.853	<0.05	0.385	>0.05
ΔC	0.731	<0.05	0.172	>0.05
CI	0.764	<0.05	0.497	>0.05
WI	−0.847	<0.05	−0.335	>0.05
BI	−0.321	>0.05	0.315	>0.05
$Hue°$	−0.520	>0.05	−0.580	>0.05
RR	0.249	>0.05	0.554	>0.05
SK	−0.443	>0.05	0.511	>0.05
ρ_{bulk}	−0.761	<0.05	−0.831	<0.05
A_O	0.420	>0.05	0.183	<0.05
A_f	0.701	<0.05	0.738	<0.05
V_O	0.499	>0.05	0.394	>0.05
V_f	0.756	<0.05	−0.002	>0.05

p-value < 0.05 means significant; p-value > 0.05 non-significant; L_O^*, a_O^* and b_O^* represent fresh samples and L^*, a^* and b^* represent dried samples as lightness, greenness/redness and blueness/yellowness; total colour difference (ΔE), chroma (ΔC), colour index (CI), whiteness index (WI), browning index (BI); Hue angle ($Hue°$); rehydration ratio RR (g/g); shrinkage SK (%) and bulk density ρ_{bulk} (g/mL); A_O: initial area of the fresh sample (mm^2); A_f: final area of the dried sample (mm^2); V_O is the initial volume of the fresh sample (mL); V_f is the final volume of the dried sample (mL).

Table 6. Summary of ANOVA results of the significant effect of infrared and hot air oven drying temperatures on calculated parameters of sliced apple samples.

Infrared Drying Temperature °C			
Calculated Parameters	**R^2**	**F-Value**	**p-Value**
L^*	0.876	8.826	<0.05
ΔE	0.832	6.179	<0.05
CI	0.815	5.499	<0.05
WI	0.877	9.917	<0.05
ρ_{bulk}	0.896	10.827	<0.05
A_f	0.894	10.586	<0.05
V_f	0.846	6.841	<0.05
Hot air oven drying temperature °C			
$Hue°$	0.878	8.973	<0.05
RR	0.876	8.821	<0.05
ρ_{bulk}	0.874	8.634	<0.05

p-value < 0.05 means significant; R^2: Coefficient of determination; L^*: Lightness of dried sample; total colour difference (ΔE); colour index (CI); whiteness index (WI); ρ_{bulk}: bulk density (g/mL); A_f: final area of the dried sample (mm^2); V_f is the final volume of the dried sample (mL); hue angle (Hue°) and rehydration ratio RR (g/g).

4. Conclusions

The drying curves of dried red delicious apple slices were described under infrared (IR) and hot air oven (OV) drying methods for drying temperatures between 40 and 80 °C at a constant drying time of 10 h. Among the fourteen thin-layer mathematical models examined, the Weibull distribution, page and logarithmic models best described the experimental drying curves. However, the Weibull distribution model was found most suitable. The suitability or the goodness of fit of the Weibull distribution model to the experimental drying curves was assessed by the smaller root mean square error (RMSE) and chi-square (χ^2) as well as greater coefficient of determination (R^2) and modelling efficiency (EF). The total colour change (ΔE), chroma (ΔC), colour index (*CI*), whiteness index (*WI*) and browning index (*BI*) showed both increasing and decreasing trends with the drying temperatures for IR and OV drying methods. All the colour indicators under IR method were higher compared to OV method. The rehydration ratio values between 1.33 ± 0.29 and 2.05 ± 0.03 increased linearly at drying temperatures from 40 °C to 70 °C but decreased at 80 °C for OV. However, for IR, the values increased from 40 °C to 50 °C and then decreased from 50 °C to 70 °C with a slight increase at 80 °C. Shrinkage values showed both increasing and decreasing trends for OV and IR methods along with the drying temperatures. There was no direct effect of the drying temperatures on the shrinkage of dried apple sliced samples under OV and IR. The bulk density of the dried apple sliced samples under OV decreased from 40 °C to 70 °C with a slight increase at 80 °C. However, compared to the IR, the values decreased from 40 °C to 50 °C and then at 80 °C but a linear increase was observed from 50 °C to 70 °C. The values ranged from 0.19 ± 0.01 to 0.46 ± 0.04 g/mL. The final area of the dried apple sliced samples for the OV method at the different drying temperatures linearly increased compared to the IR, where a slight linear trend was observed between 60 °C to 80 °C. The final volume also increased from 50 to 70 °C but then decreased at 80 °C for OV whereas a slight increase was observed for IR at 60 to 80 °C with a decrease observed from 50 to 60 °C. All the calculated parameters correlated both positively and negatively under OV and IR drying methods. The correlation values ranged from -0.216 to 0.853. The ANOVA analysis showed that only the lightness of the dried sample L^*, total colour difference (ΔE), colour index (*CI*), whiteness index (*WI*), bulk density ρ_{bulk} (g/mL), final area of the dried sample A_f (mm^2) and the final volume of the dried sample V_f (mL) were significant (*p*-value < 0.05) along with the effect of the drying temperatures. However, in comparison with the hot air oven drying method, only the hue angle, bulk density and rehydration capacity were statistically significant (*p*-value < 0.05) with the drying temperature. The results of the present study provide relevant information on sliced apple samples dried under infrared and hot air oven drying methods. Future studies would explore different and combined drying methods on physicochemical properties, drying kinetics, microstructure and specific energy consumption of different varieties of apples and other agricultural products.

Supplementary Materials: The following supporting information can be downloaded at: https://www.mdpi.com/article/10.3390/pr11103027/s1, Table S1: Calculated parameters of sliced apple samples at drying temperatures of 60 °C using infrared and hot air oven drying methods; Table S2: Calculated parameters of sliced apple samples at drying temperatures of 50 °C using infrared and hot air oven drying methods; Table S3: Calculated parameters of sliced apple samples at drying temperatures of 40 °C using infrared and hot air oven drying methods; Table S4. (a): Fitting parameter values and statistical validation metrics for drying sliced apple samples at different temperatures using infrared, IR and oven, OV drying methods; (b): Weibull distribution model fitting parameter values for drying sliced apple samples at 70 °C and 80 °C drying temperatures using infrared, IR and oven, OV drying methods; (c): Statistical validation metrics for Weibull distribution model; Table S5: ANOVA univariate results of calculated parameters of sliced apple samples under the effect of infrared drying temperatures and Table S6: ANOVA univariate results of calculated parameters of sliced apple samples under the effect of hot air oven drying temperatures; Figure S1: Column plots of bulk density ρ_{bulk} (g/mL); V_O the initial volume of fresh sample (mL) and V_f the final volume of the dried sample (mL) under infrared IR and hot air oven OV drying

temperatures; Figure S2: Column plots of A_O: initial area of the fresh sample (mm^2); A_f: final area of the dried sample (mm^2); V_O: initial volume of the fresh sample (mL) and V_f: final volume of the dried sample (mL) under infrared IR and hot air oven OV drying temperatures; Figure S3: Measured and fitted curves of dried apple sliced samples under (a) infrared and (b) hot air oven drying at 60 °C, (c) infrared and (d) hot air oven drying at 50 °C, and (e) infrared and (f) hot air oven drying at 40 °C.

Author Contributions: Conceptualisation. O.D., A.K., D.H. and Č.M.; Methodology. O.D., A.K., D.H. and Č.M.; Validation. O.D., A.K., D.H. and Č.M.; Formal analysis. O.D., A.K., D.H. and Č.M.; Data curation. O.D. and A.K.; Writing—original draft. A.K. and O.D.; Writing—review and editing. O.D., A.K., Č.M. and D.H.; Funding acquisition. D.H. All authors have read and agreed to the published version of the manuscript.

Data Availability Statement: The data presented in this study are available upon request from the corresponding author.

Conflicts of Interest: The authors declare no conflict of interest.

References

1. Musacchi, S.; Serra, S. Apple fruit quality: Overview on pre-harvest factors. *Sci. Hortic.* **2018**, *234*, 409–430. [CrossRef]
2. Barreira, J.C.M.; Arraibi, A.A.; Ferreira, I.C.F.R. Bioactive and functional compounds in apple pomace from juice and cider manufacturing: Potential use in dermal formulations. *Trends Food Sci. Technol.* **2019**, *90*, 76–87. [CrossRef]
3. Zhang, F.; Wang, T.; Wang, X.; Lu, X. Apple pomace as a potential valuable resource for full-components utilization: A review. *J. Clean. Prod.* **2021**, *329*, 129676. [CrossRef]
4. Costa, J.M.; Ampese, L.C.; Ziero, H.D.D.; Sganzerla, W.G.; Forster-Carneiro, T. Apple pomace biorefinery: Integrated approaches for the production of bioenergy, biochemicals, and value-added products—An updated review. *J. Environ. Chem. Eng.* **2022**, *10*, 108358. [CrossRef]
5. EL-Mesery, H.S.; Kamel, R.M.; Emara, R.Z. Influence of infrared intensity and air temperature on energy consumption and physical quality of dried apple using hybrid dryer. *Case Stud. Therm. Eng.* **2021**, *27*, 101365. [CrossRef]
6. Pinheiro, M.N.; Castro, L.M.M.N. Effective moisture diffusivity prediction in two Portuguese fruit cultivars (Bravo de Esmolfe apple and Madeira banana) using drying kinetics data. *Heliyon* **2023**, *9*, e17741. [CrossRef] [PubMed]
7. Shaheen, S.O.; Sterne, J.A.C.; Thompson, R.L.; Songhurst, C.E.; Margettes, B.M.; Burney, P.G.J. Dietary antioxidants and asthma in adults population-based case-control study. *Am. J. Respir. Crit. Care Med.* **2001**, *164*, 1823–1828. [CrossRef] [PubMed]
8. Kukull, W.A. An apple a day to prevent parkinson disease. *Neurology* **2012**, *78*, 1112. [CrossRef] [PubMed]
9. Khudyakov, D.; Sosnin, M.; Shorstkii, I.; Okpala, C.O.R.I. Cold filamentary microplasma combined with infrared dryer: Effects on drying efficiency and quality attributes of apple slices. *J. Food Eng.* **2022**, *329*, 111049. [CrossRef]
10. Bradford, K.J.; Dahal, P.; Asbrouck, J.V.; Kunusoth, K.; Bello, P.; Thompson, J.; Wu, F. The dry chain: Reducing postharvest losses and improving food safety in humid climates. *Trends Food Sci. Technol.* **2018**, *71*, 84–93. [CrossRef]
11. Jafari, F.; Movagharnejad, K.; Sadeghi, E. Infrared drying effects on the quality of eggplant slices and process optimization using response surface methodology. *Food Chem.* **2020**, *333*, 127423. [CrossRef] [PubMed]
12. Mohammed, S.; Edna, M.; Siraj, K. The effect of traditional and improved solar drying methods on the sensory quality and nutritional composition of fruits: A case of mangoes and pineapples. *Heliyon* **2020**, *6*, e04163. [CrossRef]
13. Sacilik, K.; Elicin, A.K. The thin layer drying characteristics of organic apple slices. *J. Food Eng.* **2009**, *73*, 281–289. [CrossRef]
14. Shewale, S.R.; Rajoriya, D.; Hebbar, H.U. Low humidity air drying of apple slices: Effect of EMR pretreatment on mass transfer parameters, energy efficiency and quality. *Innov. Food Sci. Emerg. Technol.* **2019**, *55*, 1–10. [CrossRef]
15. Aradwad, P.P.; Venkatesh, A.K.T.; Mani, I. Infrared drying of apple (*Malus demestica*) slices: Effect on drying and color kinetics, texture, rehydration, and microstructure. *J. Food Process Eng.* **2023**, *42*, e14218. [CrossRef]
16. Aral, S.; Bese, A.W. Convective drying of hawthorn fruit (*Crataegus* spp.): Effect of experimental parameters on drying kinetics, color, shrinkage, and rehydration capacity. *Food Chem.* **2016**, *210*, 577–584. [CrossRef] [PubMed]
17. Cetin, N.; Saglam, C.; Demir, B. Effects of different drying conditions on physical changes of apple (*Malus communis* L.). *MKUJAS* **2019**, *24*, 71–77.
18. Wang, H.; Liu, Z.-L.; Vidyarthi, S.K.; Wang, Q.-H.; Gao, L.; Li, B.-R.; Wei, Q.; Liu, Y.-H.; Xiao, H.-W. Effects of different drying methods on drying kinetics, physicochemical properties, microstructure, and energy consumption of potato (*Solanum tuberosum* L.) cubes. *Dry. Technol.* **2021**, *39*, 418–431. [CrossRef]
19. Guo, X.-h.; Xia, C.-Y.; Tan, Y.-R.; Chen, L.; Ming, J. Mathematical modeling and effect of various hot-air drying on mushroom (*Lentinus edodes*). *J. Integr. Agric.* **2014**, *13*, 207–216. [CrossRef]

20. Aidani, E.; Hadadkhodaparast, M.; Kashaninejad, M. Experimental and modeling investigation of mass transfer during combined infrared-vacuum drying of Hayward kiwifruits. *Food Sci. Nutr.* **2016**, *5*, 596–601. [CrossRef] [PubMed]

21. Karaaslan, S.; Ekinci, K.; Akbolat, D. Drying characteristics of sultana grape fruit in microwave dryer. *Pol. Acad. Sci.* **2017**, *IV/1*, 1317–1327.

22. Bozkir, H.; Ergun, A.R.; Serdar, E.; Metin, G.; Baysal, T. Influence of ultrasound and osmotic dehydration pretreatment on drying and quality properties of persimmon fruit. *Ultrason Sonochem.* **2019**, *54*, 135–141. [CrossRef] [PubMed]

23. Li, C.; Ren, G.; Zhang, L.; Duan, X.; Wang, Z.; Ren, X.; Chu, Q.; He, T. Effects of different drying methods on the drying characteristics and drying quality of *Cistanche deserticola*. *Food Sci. Technol.* **2023**, *184*, 115000. [CrossRef]

24. Liu, Z.-L.; Wei, Z.-P.; Vidyarthi, S.K.; Pan, Z.; Zielinska, M.; Deng, L.-Z.; Wang, Q.-H.; Wei, Q.; Xiao, H.-W. Pulsed vacuum drying of kiwifruit slices and drying process optimization based on artificial neural network. *Dry. Technol.* **2020**, *39*, 405–417. [CrossRef]

25. Cano-Lamadrid, M.; Lech, K.; Calin-Sanchez, A.; Rosas-Burgos, E.C.; Figiel, A.; Wojdylo, A.; Wasilewska, M.; Carbonell-Barrachina, A.A. Quality of pomegranate pomace as affected by drying method. *J. Food Eng.* **2018**, *55*, 1074–1082. [CrossRef]

26. Izli, G.; Izli, N.; Taskin, O.; Yildiz, G. Convective drying of kumquat slices: Comparison of different drying temperatures on drying kinetics, colour, total phenolic content and antioxidant capacity. *Lat. Am. Appl. Res.* **2018**, *48*, 37–42. [CrossRef]

27. Khaled, A.Y.; Kabutey, A.; Selvi, K.C.; Mizera, Č.; Hrabe, P.; Herák, D. Application of computational intelligence in describing the drying kinetics of persimmon fruit (*Diospyros kaki*) during vacuum and hot air drying process. *Processes* **2020**, *8*, 544. [CrossRef]

28. Izli, G.; Yildiz, G.; Berk, S.E. Quality retention in pumpkin powder dried by combined microwave-convective drying. *J. Food Sci. Technol.* **2022**, *59*, 1558–1569. [CrossRef]

29. Yildiz, G. Color, microstructure, physicochemical, textural and sensory properties with the retention of secondary metabolites in convective, microwave and freeze-dried carrot (*Daucus carota*) slices. *Br. Food J.* **2022**, *124*, 3922–3935. [CrossRef]

30. Blanco-Cano, L.; Soria-Verdugo, A.; Garcia-Gutierrez, L.M.; Ruiz-Rivas, U. Modeling the thin-layer drying process of Granny Smith apples: Application in an indirect solar dryer. *Appl. Therm. Eng.* **2016**, *108*, 1086–1094. [CrossRef]

31. Peng, J.; Yin, X.; Jiao, S.; Wei, K.; Tu, K.; Pan, L. Air jet impingement and hot air-assisted radio frequency hybrid drying of apple slices. *LWT—Food Sci. Technol.* **2019**, *116*, 108517. [CrossRef]

32. Anderson, B.A.; Singh, R.P. Modeling the thawing of frozen foods using air impingement technology. *Int. J. Refrig.* **2006**, *29*, 294–304. [CrossRef]

33. Gong, C.; Zhang, H.; Yue, J.; Miao, Y.; Jiao, S. Investigation of hot air-assisted radio frequency heating as a simultaneous dry-blanching and pre-drying method for carrot cubes. *Innov. Food Sci. Emerg. Technol.* **2019**, *56*, 102181. [CrossRef]

34. Lai, F.C.; Lai, K.W. EHD-enhanced drying with wire electrode. *Dry. Technol.* **2002**, *20*, 1393–1405. [CrossRef]

35. Martynenko, A.; Zheng, W. Electrohydrodynamic drying of apple slices: Energy and quality aspects. *J. Food Eng.* **2016**, *168*, 215–222. [CrossRef]

36. Joardder, M.U.H.; Karim, M.A. Drying kinetics and properties evolution of apple slices under convective and intermittent-MW drying. *Therm. Sci. Eng. Prog.* **2022**, *30*, 101279. [CrossRef]

37. Ceclu, L.S.; Botez, E.; Nistor, O.-V.; Andronoiu, D.G.; Mocanu, G.-D. Effect of different drying methods on moisture ratio and rehydration of pumpkin slices. *Food Chem.* **2016**, *195*, 104–109.

38. Feng, Y.; Wu, B.; Yu, X.; Yagoub, A.E.A.; Sarpong, F.; Zhou, C. Effect of catalytic infrared dry-blanching on the processing and quality characteristics of garlic slices. *Food Chem.* **2018**, *226*, 309–316. [CrossRef] [PubMed]

39. Ando, Y.; Hagiwara, S.; Nabetani, H.; Sotome, I.; Okunishi, T.; Okadome, H.; Orikasa, T.; Tagawa, A. Effects of prefreezing on the drying characteristics, structural formation and mechanical properties of microwave-vacuum dried apple. *J. Food Eng.* **2019**, *244*, 170–177. [CrossRef]

40. Lammerskitten, A.; Mykhailyk, V.; Wiktor, A.; Toepfl, S.; Nowacka, M.; Bialik, M.; Czyzewski, J.; Wiltrowa-Rajchert, D.; Parniakov, O. Impact of pulsed electric fields on physical properties of freeze-dried apple tissue. *Innov. Food Sci. Emerg. Technol.* **2019**, *57*, 102211. [CrossRef]

41. Souza da Silva, E.; Brandao, S.C.R.; Lopes da Silva, A.; Fernandes da Silva, J.H.; Coelho, A.C.D.; Azoubel, P.M. Ultrasound-assisted vacuum drying of nectarine. *J. Food Eng.* **2019**, *246*, 119–124. [CrossRef]

42. Feng, Y.; Zhou, C.; Yagoub, A.E.A.; Sun, Y.; Owusu-Ansah, P.; Yu, X.; Wang, X.; Xu, X.; Zhang, J.; Rein, Z. Improvement of the catalytic infrared drying process and quality characteristics of the dried garlic slices by ultrasound-assisted alcohol pretreatment. *LWT—Food Sci. Technol.* **2019**, *116*, 108577. [CrossRef]

43. Rojas, M.L.; Augusto, P.E.D.; Carcel, J.A. Ethanol pre-treatment to ultrasound-assisted convective drying of apple. *Innov. Food Sci. Emerg. Technol.* **2020**, *61*, 102328. [CrossRef]

44. Menges, H.O.; Ertekin, C. Mathematical modeling of thin layer dring of Golden apples. *J. Food Eng.* **2005**, *77*, 119–125. [CrossRef]

45. Meisami-asl, E.; Rafiee, S.; Keyhani, A.; Tabatabaeefar, A. Mathematical modeling of moisture content of apple slices (*Var. Golab*) during drying. *Pak. J. Nutr.* **2009**, *8*, 80–809.

46. Zhu, J.; Liu, Y.; Zhu, C.; Wei, M. Effects of different drying methods on the physical properties and sensory characteristics of apple chip snacks. *LWT—Food Sci. Technol.* **2022**, *154*, 112829. [CrossRef]

47. Das, M.; Akpinar, E.K. Determination of thermal and drying performances of the solar air dryer with solar tracking system: Apple drying test. *Case Stud. Therm. Eng.* **2020**, *21*, 100731. [CrossRef]

48. Ghinea, C.; Prisacaru, A.E.; Leahu, A. Physico-chemical and sensory quality of oven-dried and dehydrator-dried apples of the Starkrimson, golden delicious and florina cultivars. *Appl. Sci.* **2022**, *12*, 2350. [CrossRef]
49. Wang, L.; Xu, B.; Wei, B.; Zeng, R. Low frequency ultrasound pretreatment of carrot slices: Effect on the moisture migration and quality attributes by intermediate-wave infrared radiation drying. *Ultrason. Sonochem.* **2018**, *40*, 619–628. [CrossRef] [PubMed]
50. Mujumdar, A.S. *Handbook of Industrial Drying (Advances in Drying Science and Technology)*, 3rd ed.; Dekker, M., Ed.; Routledge: New York, NY, USA, 2006.
51. Sturm, B.; Vega, A.-M.N.; Hofacker, W.C. Influence of process control strategies on drying kinetics, colour and shrinkage of air dried apples. *Appl. Therm. Eng.* **2014**, *62*, 455–460. [CrossRef]
52. Thamkaew, G.; Sjoholm, I.; Galindo, F.G. A review of drying methods for improving the quality of dried herbs. *Crit. Rev. Food Sci. Nutr.* **2021**, *61*, 1763–1786. [CrossRef]
53. Hnin, K.K.; Zhang, M.; Wang, B.; Devahastin, S. Different drying methods effect on quality attributes of restructured rose powder-yam snack chips. *Food Biosci.* **2019**, *32*, 100486. [CrossRef]
54. Zhang, L.; Zhang, C.; Wei, Z.; Huang, W.; Yan, Z.; Luo, Z.; Beta, T.; Xu, X. Effects of four drying methods on the quality, antioxidant activity and anthocyanin components of blueberry pomace. *Food Prod. Process. Nutr.* **2023**, *5*, 35. [CrossRef]
55. Martynenko, A.; Janaszek, M.A. Texture changes during drying of apple slices. *Dry. Technol.* **2014**, *32*, 567–577. [CrossRef]
56. Torki-Harchegani, M.; Ghanbarian, D.; Maghsoodi, V.; Moheb, A. Infrared thin layer drying of saffron (*Crocus sativus* L.) stigmas: Mass transfer parameters and quality assessment. *Chin. J. Chem. Eng.* **2017**, *25*, 426–432. [CrossRef]
57. Huang, X.; Li, Y.; Zhou, X.; Wang, J.; Zhang, Q.; Yang, X.; Zhu, L.; Geng, Z. Prediction of apple slices drying kinetic during infrared-assisted-hot air drying by deep neural networks. *Foods* **2022**, *11*, 3486. [CrossRef] [PubMed]
58. MA 50/1.R Moisture Analyzer › Laboratory Balances—Radwag Balances And Scales, Laboratory, Industrial scales. Available online: https://radwag.com/en/ma-50r-moisture-analyzer,w1,F03,101-103-103 (accessed on 1 March 2022).
59. Nowak, D.; Lewicki, P.P. Infrared drying of apple slices. *Innov. Food Sci. Emerg. Technol.* **2004**, *5*, 353–360. [CrossRef]
60. Wu, X.-f.; Zhang, M.; Li, Z. Influence of infrared drying on the drying kinetics, bioactive compounds and flavor of *Cordyceps militaris*. *LWT—Food Sci. Technol.* **2019**, *111*, 790–798. [CrossRef]
61. Dajbych, O.; Kabutey, A.; Mizera, Č.; Herák, D. Investigation of infrared and hot air oven for drying fresh apple slices at different temperatures. In Proceedings of the International Conference on Trends in Agricultural Engineering, Prague, Czech Republic, 20–23 September 2022.
62. Bozkir, H.; Ergun, A.R. Effect of sonication and osmotic dehydration applications on the hot air drying kinetics and quality of persimmon. *LWT—Food Sci. Technol.* **2020**, *131*, 109704. [CrossRef]
63. Soares de Mendonca, K.; Correa, J.L.G.; Renato de Jesus Junqueira, J.; Cirillo, M.A.; Figueira, F.V.; Carvalho, E.E.N. Influences of convective and vacuum drying on the quality attributes of osmo-dried pequi (*Caryocar brasiliense* Camb.) slices. *Food Chem.* **2017**, *224*, 212–218. [CrossRef] [PubMed]
64. Cuccurullo, G.; Giordano, L.; Metallo, A.; Cinquanta, L. Drying rate control in microwave assisted processing of sliced apples. *Biosyst. Eng.* **2018**, *170*, 24–30. [CrossRef]
65. Nurkhoeriyati, T.; Kulig, B.; Sturm, B.; Hensel, O. The effect of pre-heating treatment and drying conditions on quality and energy consumption of hot air-dried celeriac slices: Optimisation. *Foods* **2021**, *10*, 1–19. [CrossRef] [PubMed]
66. Hussain, P.R.; Wani, I.A.; Rather, S.A.; Suradkar, P.; Ayob, O. Effect of post-processing radiation treatment on physico-chemical, microbiological and sensory quality of dried apple chips during storage. *Radiat. Phys. Chem.* **2021**, *182*, 109367. [CrossRef]
67. Bagheri, N.; Dinani, S.T. Investigation of ultrasound-assisted convective drying process on quality characteristics and drying kinetics of zucchini slices. *Heat Mass Transf.* **2019**, *55*, 2123–2163. [CrossRef]
68. Xie, Y.; Lin, Y.; Li, X.; Yang, H.; Han, J.; Shang, C.; Li, A.; Xiao, H.; Lu, F. Peanut drying: Effects of various drying methods on drying kinetic models, physicochemical properties, germination characteristics, and microstructure. *Inf. Process. Agric.* **2022**. [CrossRef]
69. Xiao, H.W.; Pang, C.L.; Wang, L.H.; Bai, J.W.; Yang, W.X.; Gao, Z.J. Drying kinetics and quality of Monukka Seedless grapes dried in an air–impingement jet dryer. *Biosyst. Eng.* **2010**, *105*, 233–240. [CrossRef]
70. Cui, Z.W.; Li, C.Y.; Song, C.F.; Song, Y. Combined microwave vacuum and freeze drying of carrot and apple chips. *Dry. Technol.* **2008**, *26*, 1517–1523. [CrossRef]
71. Majdi, H.; Esfahani, J.A.; Mohebbi, M. Optimization of convective drying by response surface methodology. *Comput. Electron. Agric.* **2019**, *156*, 574–584. [CrossRef]
72. Zhu, Y.; Pan, Z.; McHugh, T.H.; Barrett, D.M. Processing and quality characteristics of apple slices processed under simultaneous infrared dry-blanching and dehydration with intermittent heating. *J. Food Eng.* **2010**, *97*, 8–16. [CrossRef]
73. Goula, A.M.; Adamopoulos, K.G. Spray drying of tomato pulp in dehumidified air: II. The effect on powder properties. *J. Food Eng.* **2005**, *66*, 35–42. [CrossRef]
74. Westerman, P.W.; White, G.M.; Ross, I.J. Relative humidity effect on the high temperature drying of shelled corn. *Trans. ASABE* **1973**, *16*, 1136–1139. [CrossRef]
75. Onwude, D.I.; Hashim, N.; Janius, R.B.; Nawi, N.M.; Abdan, K. Modeling the thin layer drying of fruits and vegetables: A review. *Compr. Rev. Food Sci. Food Saf.* **2016**, *15*, 599–618. [CrossRef]
76. Page, G.E. Factors Influencing the Maximum Rates of Air Drying Shelled Corn in Thin Layers. Master's Thesis, Department of Mechanical Engineering, Prude University, West Lafayette, IN, USA, 2009.

77. Yaldiz, O.; Ertekin, C. Thin layer solar drying of some different vegetables. *Dry. Technol.* **2001**, *19*, 583–596. [CrossRef]

78. Yagcioglu, A.; Degirmencioglu, A.; Cagatay, F. Drying characteristics of laurel leaves under different conditions. In Proceedings of the 7th International Congress on Agricultural Mechanization and Energy, Adana, Turkey, 29 October–1 November 2023; Bascetincelik, A., Ed.; Faculty of Agriculture, Cukorova University: Adana, Turkey, 1999; pp. 565–569.

79. Yaldiz, O.; Ertekin, C.; Uzun, H.I. Mathematical modeling of thin layer solar drying of Sultana grapes. *Energy.* **2001**, *26*, 457–465. [CrossRef]

80. Rahman, M.S.; Perera, C.O.; Thebaud, C. Desorption isotherm and heat pump drying kinetics of peas. *Food Int. Res.* **1998**, *30*, 485–491. [CrossRef]

81. Ozdemir, M.; Devres, Y.O. The thin layer drying characteristics of hazelnuts during roasting. *J. Food Eng.* **1999**, *42*, 225–233. [CrossRef]

82. Verma, L.R.; Bucklin, R.A.; Endan, J.B.; Wratten, F.T. Effects of drying air parameters on rice drying models. *Trans. ASAE* **1985**, *28*, 296–301. [CrossRef]

83. Karathanos, V.T. Determination of water content of dried fruits by drying kinetics. *J. Food Eng.* **1999**, *39*, 337–344. [CrossRef]

84. Midilli, A.; Kucuk, H.; Yapar, Z. A new model for single layer drying of some vegetables. *Dry. Technol.* **2002**, *20*, 1503–1513. [CrossRef]

85. Babalis, S.T.; Papanicolaou, E.; Kyriakis, N.; Belessiotis, V.G. Evaluation of thin layer drying models for describing drying kinetics of figs (*Ficus carica*). *J. Food Eng.* **2006**, *75*, 205–214. [CrossRef]

86. Alibaş, I. Microwave drying of strawberry slices and the determination of the some quality parameters. *J. Agric. Mach. Sci.* **2012**, *8*, 161–170.

87. Goyal, R.K.; Kingsly, A.R.P.; Manikantan, M.R.; Llyas, S.M. Mathematical modelling of thin layer drying kinetics of plum in a tunnel dryer. *J. Food Eng.* **2007**, *79*, 176–180. [CrossRef]

88. Boy, V.; Mlayah, S.; Giblaine, M.; Lemee, Y.; Lanoiselle, J.-L. A case study at turbulent free jet flows issuing from rectangular slots on process performances and quality of hot-air-dried apple. *Processes* **2021**, *9*, 1900. [CrossRef]

89. Statsoft Inc. *STATISTICA for Windows*; Statsoft Inc.: Tulsa, OK, USA, 2013.

90. Reimann, C.; Filzmoser, P.; Garrett, R.; Dutter, R. *Statistical Data Analysis Explained: Applied Environmental Statistics with R*; John Wiley & Sons Ltd.: Chichester, UK, 2008.

91. Edjabou, M.E.; Martin-Fernandez, J.A.; Scheutz, C.; Astrup, T.F. Statistical analysis of solid waste composition data: Arithmetic mean, standard deviation and correlation coefficients. *Waste Manag.* **2017**, *69*, 13–33. [CrossRef]

92. Cruz, A.C.; Guiné, R.P.F.; Gonçalves, J.C. Drying Kinetics and Product Quality for Convective Drying of Apples (cvs. Golden Delicious and Granny Smith). *Int. J. Fruit Sci.* **2015**, *15*, 54–78. [CrossRef]

93. Lechtanska, J.M.; Szadzinska, J.; Kowalski, S.J. Microwave and infrared-assisted convective drying of green pepper: Quality and energy considerations. *Chem. Eng. Process.* **2015**, *98*, 155–164. [CrossRef]

94. Alibas, I.; Yilmaz, A. Microwave and convective drying kinetics and thermal properties of orange slices and effect of drying on some phytochemical parameters. *J. Therm. Anal. Calorim.* **2021**, *147*, 8301–8321. [CrossRef]

95. Vishwanathan, K.H.; Giwari, G.K.; Hebbar, H.U. Infrared assisted dry-blancing and hybrid drying of carrot. *Food Bioprod. Process.* **2013**, *91*, 89–94. [CrossRef]

96. Baysal, T.; Icier, F.; Ersus, S.; Yildiz, H. Effects of microwave and infrared drying on the quality of carrot and garlic. *Eur. Food Res. Technol.* **2003**, *218*, 68–73. [CrossRef]

97. Vishwanathan, K.H.; Hebbar, H.U.; Raghavarao, K.S.M.S. Hot air assisted infrared drying of vegetables and its quality. *Food Sci. Technol. Res.* **2010**, *15*, 381–388. [CrossRef]

98. Lewicki, P.P.; Jakubczyk, E. Effect of hot air temperature on mechanical properties of dried apples. *J. Food Eng.* **2004**, *64*, 307–314. [CrossRef]

99. Bai, Y.; Rahman, M.S.; Perera, C.O.; Smith, B.; Melton, L.D. Structural changes in apple rings during convection air-drying with controlled temperature and humidity. *J. Agric. Food Chem.* **2002**, *50*, 3179–3185. [CrossRef]

100. Dhurve, P.; Arora, V.K.; Yadav, D.K.; Malakar, S. Drying kinetics, mass transfer parameters, and specific energy consumption analysis of watermelon seeds dried using the convective dryer. *Mater. Today* **2020**, *50*, 926–932. [CrossRef]

101. Murugesan, K.; Thomas, H.R.; Cleall, P.J. An investigation of the influence of two-stage drying conditions on convective drying of porous materials. *Int. J. Num. Meth. Heat Fluid Flow* **2002**, *12*, 29–46. [CrossRef]

102. Yu, X.L.; Zielinska, M.; Ju, H.Y.; Mujumdar, A.S.; Duan, X.; Gao, Z.J.; Xiao, H.W. Multistage relative humidity control strategy enhances energy and exergy efficiency of convective drying of carrot slices. *Int. J. Heat Mass Transf.* **2020**, *149*, 119231. [CrossRef]

103. Doymaz, I. Drying behaviour of green beans. *J. Food Eng.* **2005**, *69*, 161–165. [CrossRef]

104. Onwude, I.; Hashim, N.; Abdan, K.; Janius, R.; Chen, G. The effectiveness of combined infrared and hot-air drying strategies for sweet potato. *J. Food Eng.* **2019**, *241*, 75–87. [CrossRef]

105. Bitencourt, B.S.; Correa, J.L.G.; Carvalho, G.R.; Augusto, P.E.D. Valorization of pineapple pomace for food or feed: Effects of pre-treatment with ethanol on convective drying and quality properties. *Waste Biomass Valori.* **2022**, *13*, 2253–2266. [CrossRef]

106. Chia, Z.B.; Putranto, A.; Chen, X.D.; Onwude, D.I. Combined infrared and hot air drying (IR-HAD) of sweet potato explored using a multiphase model: Application of reaction engineering approach. *Dry. Technol.* **2022**, *40*, 1629–1638. [CrossRef]

107. Simal, S.; Mulet, A.; Tarrazo, J.; Rossello, C. Drying models for green peas. *Food Chem.* **1996**, *55*, 121–128. [CrossRef]

108. Panchariya, P.C.; Popovic, D.; Sharma, A.L. Thin-layer modelling of black tea drying process. *J. Food Eng.* **2002**, *52*, 349–357. [CrossRef]
109. Moradi, M.; Niakousari, M.; Khaneghah, A.M. Kinetics and mathematical modeling of thin layer drying of osmo-treated Aloe vera (*Aloe barbadensis*) gel slices. *J. Food Process Eng.* **2019**, *42*, e13180. [CrossRef]
110. Hasan, T. Simple modelling of infrared drying of fresh apple slices. *J. Food Eng.* **2005**, *71*, 311–323.